Geological Society of America
3300 Penrose Place
P.O. Box 9140
Boulder, CO 80301
(303) 447-2020 • fax 303-357-1073
www.geosociety.org

Geological Society of America
Special Paper 404
2006

Application of carbonate cyclostratigraphy and borehole geophysics to delineate porosity and preferential flow in the karst limestone of the Biscayne aquifer, SE Florida

Kevin J. Cunningham
Robert A. Renken
Michael A. Wacker
Michael R. Zygnerski
U.S. Geological Survey, Fort Lauderdale, Florida 33315, USA
Edward Robinson
University of West Indies, Kingston, Jamaica
Allen M. Shapiro
G. Lynn Wingard
U.S. Geological Survey, Reston, Virginia 20192, USA

ABSTRACT

Combined analyses of cores, borehole geophysical logs, and cyclostratigraphy produced a new conceptual hydrogeologic framework for the triple-porosity (matrix, touching-vug, and conduit porosity) karst limestone of the Biscayne aquifer in a 0.65 km^2 study area, SE Florida. Vertical lithofacies successions, which have recurrent stacking patterns, fit within high-frequency cycles. We define three ideal high-frequency cycles as: (1) upward-shallowing subtidal cycles, (2) upward-shallowing paralic cycles, and (3) aggradational subtidal cycles. Digital optical borehole images, tracers, and flow meters indicate that there is a predictable vertical pattern of porosity and permeability within the three ideal cycles, because the distribution of porosity and permeability is related to lithofacies. Stratiform zones of high permeability commonly occur just above flooding surfaces in the lower part of upward-shallowing subtidal and paralic cycles, forming preferential groundwater flow zones. Aggradational subtidal cycles are either mostly high-permeability zones or leaky, low-permeability units. In the study area, groundwater flow within stratiform high-permeability zones is through a secondary pore system of touching-vug porosity principally related to molds of burrows and pelecypods and to interburrow vugs. Movement of a dye-tracer pulse observed using a borehole fluid-temperature tool during a conservative tracer test indicates heterogeneous permeability. Advective movement of the tracer appears to be most concentrated within a thin stratiform flow zone contained within the lower part of a high-frequency cycle, indicating a distinctly high relative permeability for this zone. Borehole flow-meter measurements corroborate the relatively high permeability of the flow zone. Identification and mapping of such high-permeability flow

Cunningham, K.J., Renken, R.A., Wacker, M.A., Zygnerski, M.R., Robinson, E., Shapiro, A.M., and Wingard, G.L., 2006, Application of carbonate cyclostratigraphy and borehole geophysics to delineate porosity and preferential flow in the karst limestone of the Biscayne aquifer, SE Florida, *in* Harmon, R.S., and Wicks, C., eds., Perspectives on karst geomorphology, hydrology, and geochemistry—A tribute volume to Derek C. Ford and William B. White: Geological Society of America Special Paper 404, p. 191–208, doi: 10.1130/2006.2404(16).

zones is crucial to conceptualization of karst groundwater flow within a cyclostratigraphic framework. Many karst aquifers are included in cyclic platform carbonates. Clearly, a cyclostratigraphic approach that translates carbonate aquifer heterogeneity into a consistent framework of correlative units will improve simulation of karst groundwater flow.

Keywords: carbonate cyclostratigraphy, borehole geophysics, karst, hydrogeology, Florida.

INTRODUCTION

A fundamental problem in the simulation of karst groundwater flow and solute transport is how best to represent aquifer heterogeneity as defined by the spatial distribution of porosity and permeability. By definition, karst carbonate aquifers contain dissolution-generated conduits that allow rapid movement of groundwater, often in turbulent flow (White, 2002). Carbonate conduit flow systems pose a unique problem because of complex variations in lithofacies and diagenetic history that have contributed to its heterogeneity. Karst flow models can improve if conceptual hydrogeologic models accurately delineate the distribution of conduits and aquifer matrix (White, 1999). This is especially true of Paleozoic karst aquifers, which can include pipe-like conduits that may be single caves or have a complex branch-work pattern (White and White, 2001). In younger Cretaceous and Cenozoic karst aquifers, zones of high porosity have been shown to occur within or equivalent to small-scale depositional cycles (Hovorka et al., 1996, 1998; Budd, 2001; Ward et al., 2003; Budd and Vacher, 2004; Cunningham et al., 2004b, 2004c, 2006), indicating a well-defined cyclostratigraphic framework can be used to map the three-dimensional aspects of karst groundwater flow.

The purpose of this paper is to delineate the lithofacies, depositional environments, cyclostratigraphy, porosity, and permeability of the karst limestone of the Pleistocene Biscayne aquifer in north-central Miami-Dade County, Florida (Figs. 1 and 2). This paper demonstrates how carbonate cyclostratigraphy is crucial to the definition of spatial distribution of porosity and permeability within a triple-porosity (matrix, touching-vug, and conduit porosity) karst aquifer. This study is part of a more comprehensive investigation to assess the efficacy of karst limestone underlying the Miami-Dade County's Northwest Well Field (Fig. 1) to attenuate movement of pathogenic organisms (Renken et al., 2005). County officials are concerned that proposed expansion of extractive limestone rock mines near the well field will increasingly influence the ambient quality of groundwater. The U.S. Environmental Protection Agency requires public water supplies derived from "ground water under direct influence of surface water" use enhanced disinfection and filtration treatment processes to remove pathogenic organisms (Federal Register Notice, 2000).

The application of cyclostratigraphy has proven critical to the development of a new conceptual hydrogeologic framework within the Biscayne aquifer (Cunningham et al., 2004b, 2004c, 2006). In this paper, a high-resolution cyclostratigraphic model throughout the entire thickness of the karstic Biscayne aquifer is used to select consistent, correlative flow zones between an injection well and the point of tracer recovery, a Northwest Well Field production well. This framework serves as the physical basis for scoping, designing, and executing a series of conservative and colloidal tracer tests (Renken et al., 2005).

STUDY AREA AND METHODS

The study area is contained within an ~0.65 km^2 area of the municipal Northwest Well Field in Miami-Dade County, SE Florida (Fig. 1). Located within the Lake Belt area (Fig. 1C), the Northwest Well Field is the largest drinking-water well field in Florida. Fifteen water-supply wells withdraw potable groundwater from the Biscayne aquifer (Fig. 2) and have a permitted yield of ~587,000 m^3 of water per day. The Lake Belt area is a multi-use region that annually supplies one-half of the limestone used in Florida, serves as a source of municipal drinking water, and forms a buffer between Everglades wetland areas to the west and high-density urban areas to the east. The highly transmissive Biscayne aquifer includes the Pleistocene Fort Thompson Formation and Miami Limestone underlying the Northwest Well Field (Fig. 2).

In this study, we analyzed core samples (10.2 cm in diameter, 139 m cumulative length) obtained from five core holes. Three test core holes were drilled under the direction of the Miami-Dade County Water and Sewer Department in 1998 (test core holes adjacent to production wells S-3168, S-3169, and S-3170), and the U.S. Geological Survey (USGS) supervised drilling of two continuously cored test wells (observation well G-3772 and injection well G-3773) during 2002 (Figs. 1C and 1D). The distance of a transect including these five wells is ~1.7 km, with well-to-well distances of separation ranging from 0.07 to 0.83 km. The five cores were slabbed and visually analyzed using a 10× magnification hand lens and binocular microscope. Standard transmitted-light petrography aided examination of 111 thin sections of core samples from the G-3772, G-3773, and S-3169 wells (Figs. 1C and 1D). Core and thin-section analyses determined lithofacies, vertical patterns of lithofacies, sedimentary structures, cycle boundaries, and assessed lateral correlation or variability of these features. Lithofacies were defined by allochem types, fabric, sedimentary structures, bedding type,

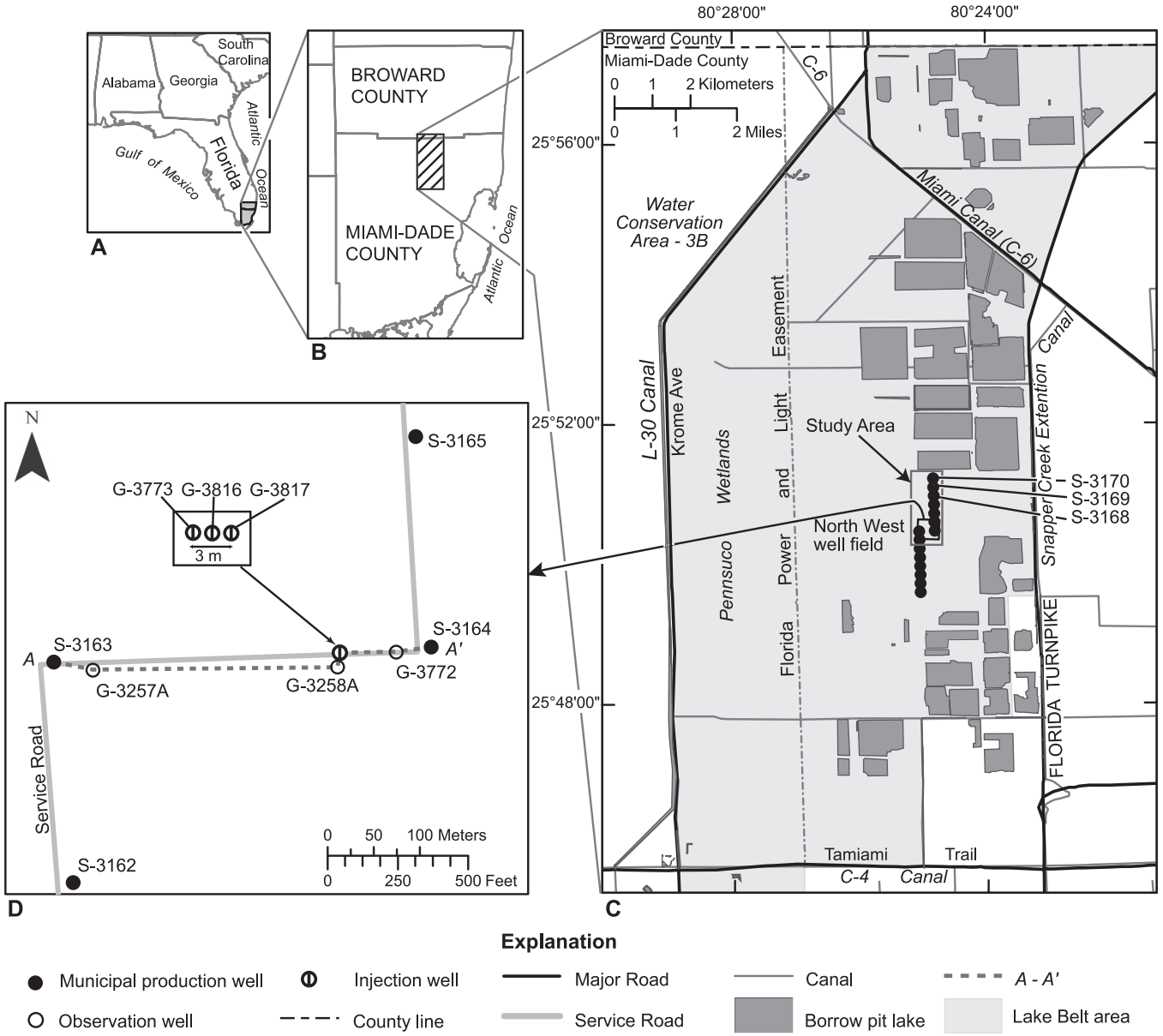

Figure 1. Locality of study area. (A) Southeastern USA and location of Miami-Dade and Broward Counties, Florida. (B) Location of the Lake Belt area in SE Florida. (C) Location of the study area within the Northwest Well Field and much of the Lake Belt area. (D) Details of part of the study area, including location of injection, observation, and some of the municipal supply wells within the Northwest Well Field.

and diagenetic features, using a combination of classification schemes and terminology from Dunham (1962), Embry and Klovan (1971), and Lucia (1999). Relationships between lithofacies and petrophysical properties (porosity and permeability) were assessed using methods of Lucia (1995, 1999).

A Mount Sopris OBI-40 digital optical logging tool produced continuous digital images of the borehole walls in the G-3772 and G-3773 core holes. These images were used to appraise the distribution of highly porous stratal intervals not recovered in the core record and to image the borehole cyclostratigraphy and associated pore network. Four air-rotary wells (G-3257A, G-3258A, G-3816, and G-3817), drilled under supervision of the USGS, were optically logged for this study, and continuous images of their borehole walls were compared to the cyclostratigraphy and pore systems observed in the cored wells (Fig. 1D). Observation wells G-3257A and G-3258A were drilled in 1983, and borehole injection wells G-3816 and G-3817 were completed in 2003. Percent vuggy porosity observed in digital borehole images in the G-3772 and G-3773 wells was calculated employing a technique described in Cunningham et al. (2004a). Cyclostratigraphic correlations were corroborated by comparison to larger-scale, inclusive hydro-

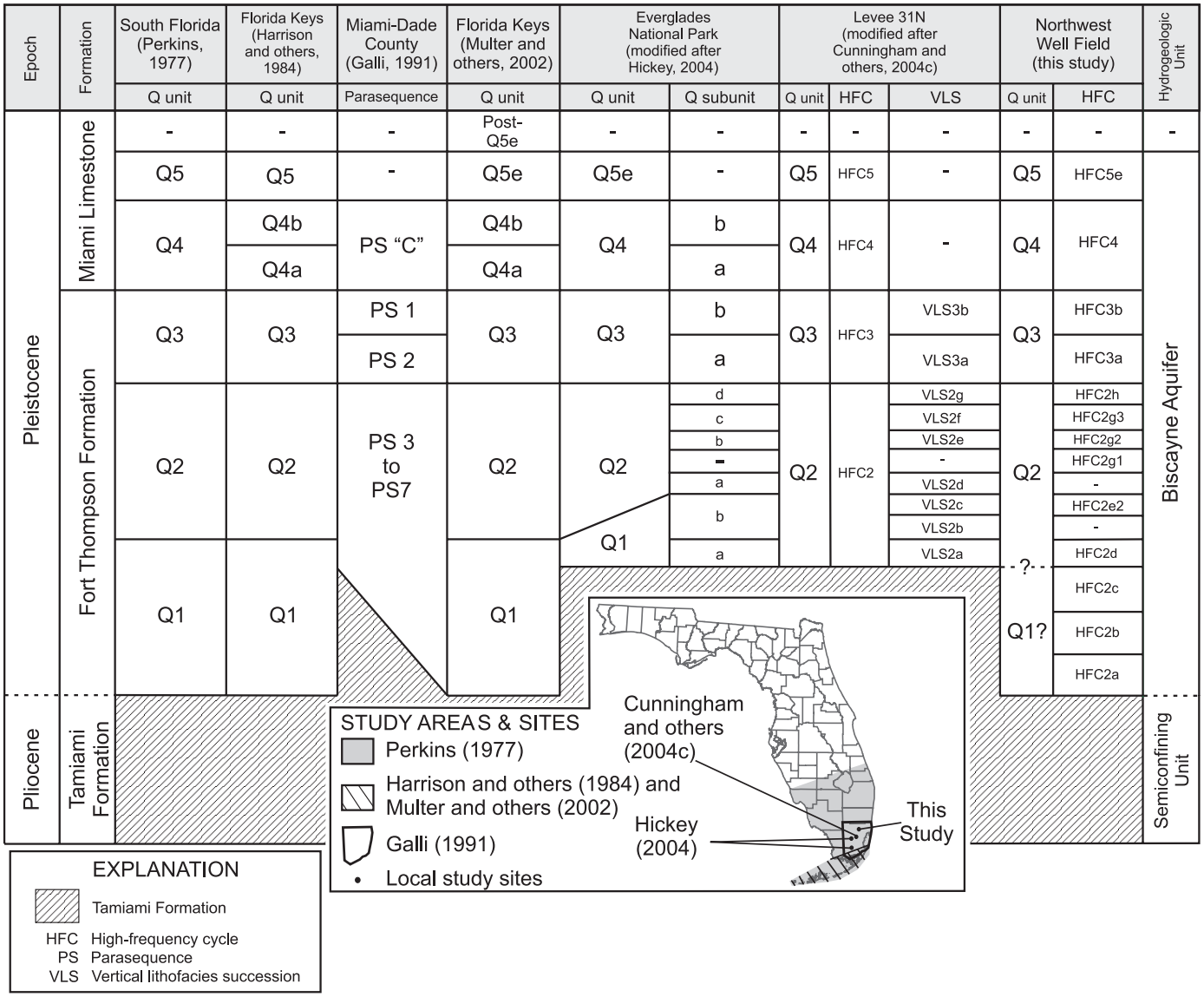

Figure 2. Correlation of ages, formations, stratigraphy, and hydrogeologic units of the Tamiami Formation, Fort Thompson Formation, and Miami Limestone from various authors and this study.

geologic and cyclostratigraphic relations currently being established for the entire Lake Belt area (Cunningham et al., 2004b, 2004c, 2006).

Taxonomy of mollusks and foraminifera from selected lithofacies was determined to assist in interpretation of paleoenvironments. Mollusks from 13 core samples obtained from the S-3168 and S-3170 test core holes (Fig. 1C) were prepared and identified. Preservation of most of the mollusks present in the samples was as either molds or casts. Core samples were initially examined under a binocular microscope to observe diagnostic characteristics of the molluskan taxonomy and to compare with published documents (e.g., Mansfield, 1939; Olsson and Harbison, 1953; DuBar, 1958; Olsson and Petit, 1964; Abbott, 1974; Portell et al., 1992). Where appropriate, clay squeezes or latex casts were made of the molluskan molds to help in identification. Many molluskan species present in the Pleistocene units of south Florida are extant or represented by close relatives, so interpretation of paleoenvironmental settings is based on living fauna. Publications by Perry and Schwengel (1955), Warmke and Abbott (1961), Abbott (1974), Andrews (1977), and Brewster-Wingard et al. (2001) support our paleoenvironmental interpretations. Information contained in Bock et al. (1971) and Poag (1981) aided our benthic foraminiferal identifications at the genus level for the 111 thin sections. Data described in Bock et al. (1971), Rose and Lidz (1977), Poag (1981), and Lidz and Rose (1989) assisted our interpretation of paleoenvironmental conditions based on foraminiferal taxonomy.

Data combined from borehole fluid-conductivity and fluid-temperature logs, caliper logs, digital borehole image logs, and borehole flow-meter measurements delineated intervals with inflow or outflow from boreholes. Considered together, these logs provided information on formation permeability (Keys, 1990; Paillet, 2004). Fluid-conductivity logs have been used to assess changes in concentration of dissolved solids in the borehole fluid column (Keys, 1990). A sharp change in borehole fluid conductivity or fluid temperature or both can identify borehole intervals showing inflow or outflow (Keys, 1990). Caliper and digital borehole image data used in combination with borehole-fluid logs can identify potential high-permeability flow zones. A suite of caliper, digital borehole image, borehole fluid-conductivity, and fluid-temperature logs were obtained for the G-3772 observation well and G-3773 injection well. In the G-3773 well, a Century Geophysical Corporation electromagnetic flow meter was used in static (stationary measurements) and trolling modes (measurements while the tool moves up or down the well bore) to measure vertical borehole groundwater flow under stressed and ambient conditions. A 10.2-cm-diameter suction-lift centrifugal pump withdrawing at an average rate of 454 L/min was used in the G-3773 well to produce stressed conditions during a single-well flow-meter test. Ambient measurements were collected at the G-3773 well during unstressed conditions.

The injection well G-3773, observation well G-3772, and a well-field production well (S-3164) were used during a forced-gradient, convergent tracer test using a fluorescent dye and deuterium in April 2003 (Fig. 1D). The G-3816, G-3817, G-3772, and S-3164 wells were used for additional tracer tests, using bromide, dissolved gas, deuterium, and colloidal particles, conducted in February and March 2004 (Fig. 1D). This study uses only results from the 2003 test; however, Renken et al. (2005) discuss some results of the 2004 tests.

LITHOFACIES AND DEPOSITIONAL ENVIRONMENTS

Lithofacies and vertical lithofacies successions (Kerans and Tinker, 1977) are the two principal lithostratigraphic elements identified in this study. A vertical lithofacies succession is a distinct stack of lithofacies that records upward shallowing or an amalgamation of a persistent environment as accommodation fills within a cycle-scale relative sea-level rise (cf. Kerans and Tinker, 1997). We arranged lithofacies into vertical lithofacies successions that represent either upward-shallowing units or units composed entirely or mostly of a distinct lithofacies representative of a single prevailing depositional water depth (Fig. 3). Five depositional environments characterize the rocks of the Fort Thompson Formation and Miami Limestone.

Lithofacies

Lithofacies are the fundamental descriptive rock components of this study. Fifteen lithofacies delineate the sedimentary rocks that form the Fort Thompson Formation and Miami Limestone at the Northwest Well Field. If a rock was composed of a significant amount of quartz sand grains, but less than 50%, then "sandy" is used as the prefix to the lithofacies type. "Touching-vugs," a prefix to a lithofacies type, refers to vuggy porosity that forms an interconnected pore system (Lucia, 1999). The 15 lithofacies include: (1) peloid packstone and grainstone, (2) peloid wackestone and packstone, (3) *Planorbella* floatstone and rudstone, (4) pedogenic limestone (laminated calcrete, massive calcrete, and root-mold limestone), (5) mudstone and wackestone, (6) laminated peloid packstone and grainstone, (7) skeletal packstone and grainstone, (8) sandy skeletal packstone and grainstone, (9) coral framestone, (10) pelecypod floatstone and rudstone, (11) sandy pelecypod floatstone and rudstone, (12) touching-vug pelecypod floatstone and rudstone, (13) sandy touching-vug floatstone and rudstone, (14) skeletal quartz sandstone, and (15) conglomerate (Figs. 3 and 4). Cunningham et al. (2004b) contains detailed descriptions of these lithofacies and inferred environments of deposition, although some lithofacies terminology and definitions of depositional environments are modified herein. For example, the gastropod floatstone and rudstone lithofacies used in Cunningham et al. (2004b, 2004c) has been renamed *Planorbella* floatstone and rudstone in this study.

Depositional Environments

Five major carbonate depositional environments characterize the Fort Thompson Formation and Miami Limestone in the study area (Figs. 3, 4, and 5). In a generally regressive succession, these include: (1) platform margin to outer platform, (2) open-marine platform interior, (3) restricted platform interior, (4) brackish platform interior, and (5) freshwater terrestrial environments. Rock fabric and texture, faunal constituents, sedimentary structures, and relation to surfaces bounding vertical lithofacies successions were the basis for interpretation of the five depositional environments for the rocks of the Fort Thompson Formation and Miami Limestone. In the study area, all five depositional environments were recognized in the Fort Thompson Formation (Fig. 5); however, only the open-marine platform interior environment is representative of lithofacies contained in the Miami Limestone.

Platform Margin to Outer Platform

The four lithofacies that distinguish the platform margin to outer platform environments include coral (*Montastrea*) framestone, conglomerate, sandy skeletal packstone and grainstone, and sandy pelecypod floatstone and rudstone lithofacies. The grainy lithofacies contain amphistiginids, which prefer areas of reef growth in the platform margin of the modern south Florida platform, and patch reefs and nearby environments not far (possibly a few kilometers) from the platform margin (Rose and Lidz, 1977). The platform margin to outer platform environments are a notable exception because they only occur at the base of the Fort Thompson Formation in the study area. Rocks representative of

Upward-Shallowing Subtidal Cycle (Fort Thompson Fm)

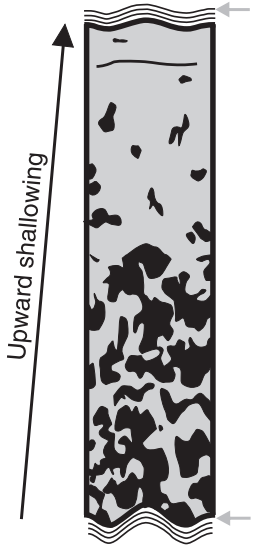

Major lithofacies	Depositional environment	Pore class	Ground-water flow type
Skeletal packstone and grainstone, sandy skeletal packstone and grainstone, pelecypod floatstone and rudstone, sandy pelecypod floatstone and rudstone	Restricted platform interior to open-marine platform interior	II	Diffuse-carbonate flow
Touching-vug pelecypod floatstone and rudstone, sandy touching-vug pelecypod floatstone and rudstone	Open-marine platform interior	I	Mainly touching-vug and less common conduit flow

Upward-Shallowing Paralic Cycle (Fort Thompson Fm)

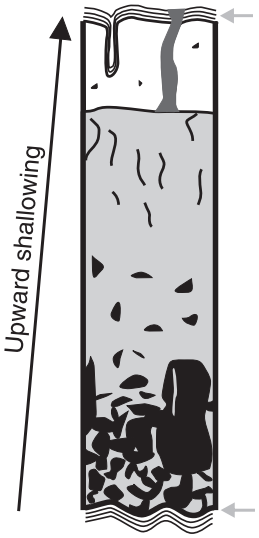

Major lithofacies	Depositional environment	Pore class	Ground-water flow type
Planorbella floatstone and rudstone and/or mudstone and wackestone	Freshwater and/or brackish platform interior	III	Leaky, low permeability
Skeletal packstone and grainstone, sandy skeletal packstone and grainstone, pelecypod floatstone and rudstone, sandy pelecypod floatstone and rudstone	Restricted platform interior to open-marine platform interior	II	Diffuse-carbonate flow
Touching-vug pelecypod floatstone and rudstone, sandy touching-vug pelecypod floatstone and rudstone	Open-marine platform interior	I	Mainly touching-vug and less common conduit flow

Aggradational Subtidal Cycles (Miami Limestone)

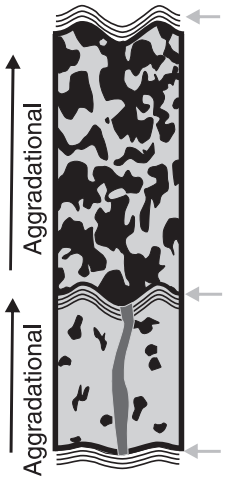

Major lithofacies	Depositional environment	Pore class	Ground-water flow type
Peloid packstone and grainstone	Open-marine platform interior	I	Mainly touching-vug and less common conduit flow
Peloid wackestone and packstone		III	Leaky, low permeability

EXPLANATION

- MICRITE-DOMINATED MATRIX
- GRAIN-RICH OR GRAIN-DOMINATED MATRIX
- IRREGULAR VUGS
- THIN ROOT MOLDS
- LAMINATED CALCRETE
- FLOODING SURFACE
- MOLDIC AND IRREGULAR VUGS
- VERTICAL VUGS

Figure 3. Idealized fifth-order cycles (Table 2) for the Fort Thompson Formation and Miami Limestone. Note the relations between lithofacies, depositional environments, porosity (pore classes), and groundwater-flow types. In terms of aquifer characterization, important points are that the most porous and permeable parts (pore classes) of the two upward-shallowing cycles are just above the flooding surface in the lower part of the cycles, and the aggradational cycles have a generally regular vertical distribution of vuggy porosity throughout the cycles.

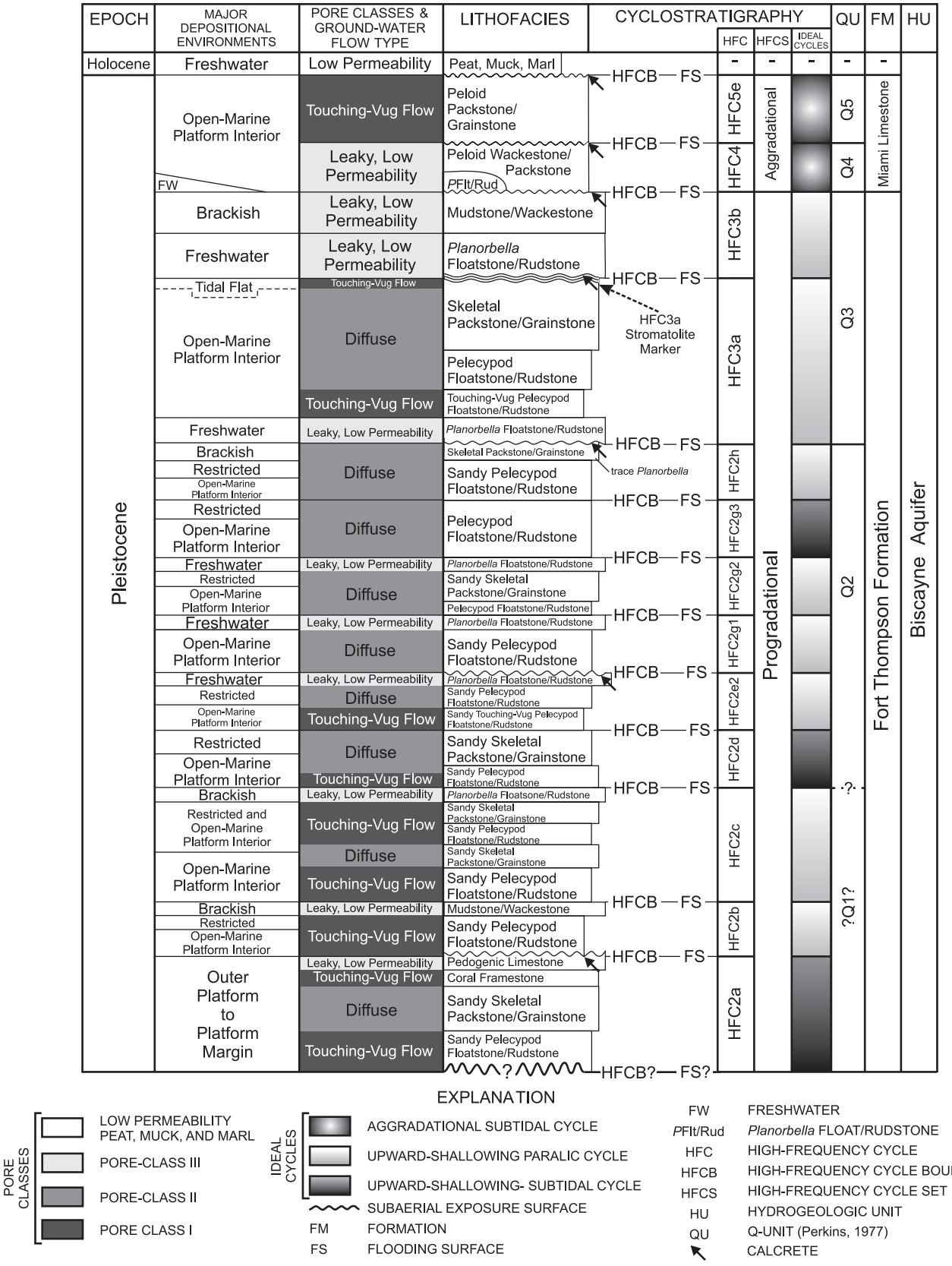

Figure 4. Conceptual hydrogeologic column for the Northwest Well Field including ages, major depositional environments, groundwater-flow types, pore classes, lithofacies, cyclostratigraphy, Q-units of Perkins (1977), formations, and hydrogeologic units.

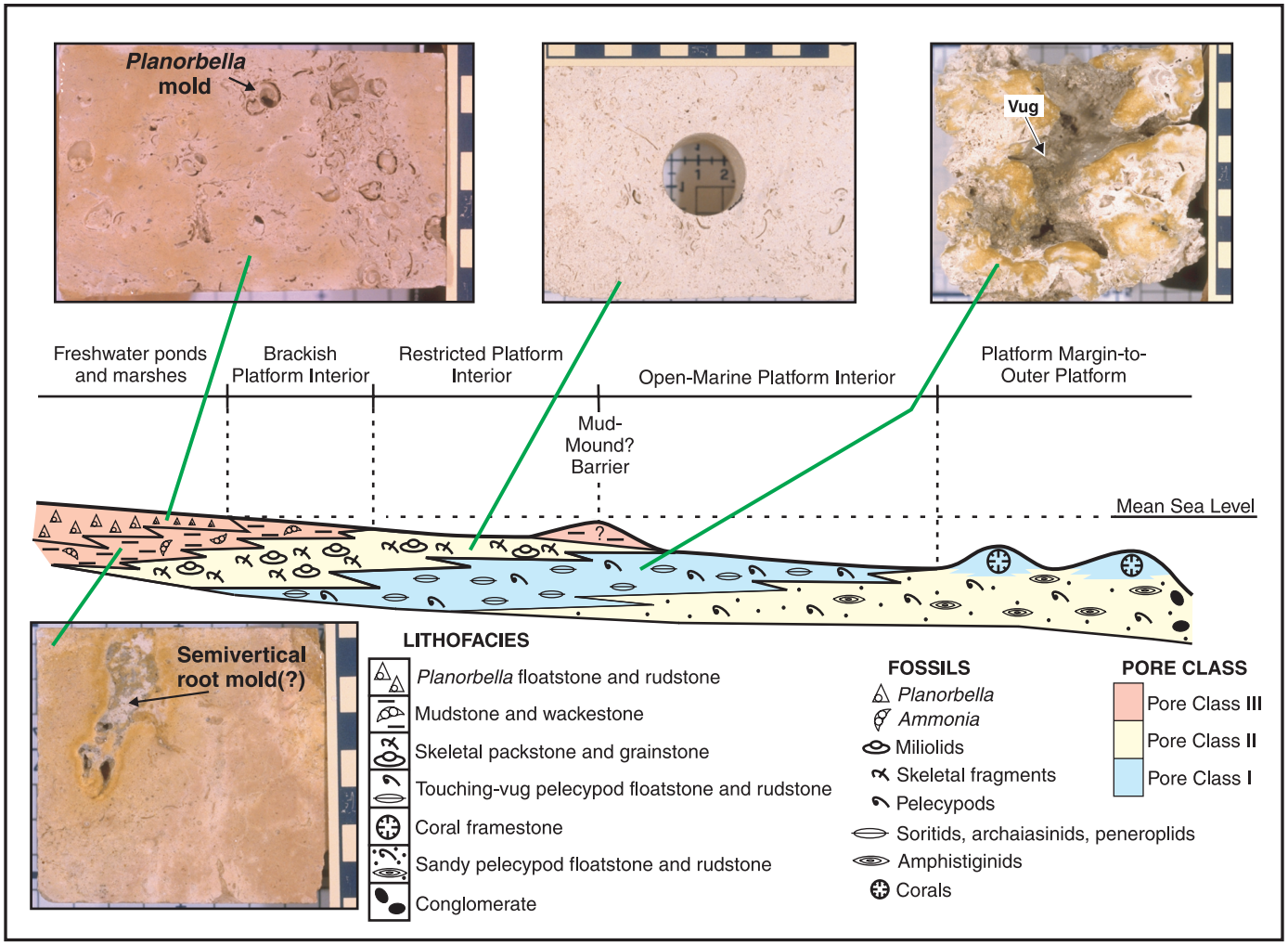

Figure 5. Conceptual facies model showing relations between major lithofacies, depositional environments, and pore classes for the Fort Thompson Formation at the Northwest Well Field (Figs. 1 and 2). Five main depositional environments include platform margin to outer platform, open-marine platform interior, restricted platform interior, brackish platform interior, and freshwater terrestrial (ponds and marshes) environments. The platform margin to outer platform depositional environments are a notable exception because they are representative of only the lowermost high-frequency cycle (HFC2a) of the Fort Thompson Formation (Fig. 4). Four photographs of characteristic slabbed-core samples from the Fort Thompson Formation illustrate some of the carbonate textures and diagenetic features associated with key lithofacies. Each incremental color change represents 1 cm on the scale bars.

these environments overlie quartz sand and quartz-sand–rich limestone of the Tamiami Formation (Fig. 2), which Cunningham et al. (2006) suggested indicate a middle-ramp environment. Common to the sand and limestone of the Tamiami Formation are amphistiginids, globigerinids, and other planktonic foraminifers indicative of relatively deep water. Together, the rocks of the uppermost Tamiami Formation and basal Fort Thompson Formation are consistent with upward shallowing.

Open-Marine Platform Interior

Overlying the platform margin to outer platform depositional facies in the lowermost Fort Thompson Formation is open-marine platform interior depositional facies, further suggesting upward shallowing and platform progradation within the lower Fort Thompson Formation (Fig. 4). For the Fort Thompson Formation, lithofacies characteristic of the open-marine platform interior depositional environment include touching-vug pelecypod floatstone and rudstone, sandy touching-vug pelecypod floatstone and rudstone, skeletal packstone and grainstone, and sandy skeletal packstone and grainstone lithofacies. Common to these lithofacies are benthic foraminifers (soritids, archaiasinids, and peneroplids) that suggest deposition in an open-marine platform interior, similar to the modern platform interior of southern Florida that is seaward of the present-day islands of the Florida Keys (Rose and Lidz, 1977; Lidz and Rose, 1989). These lithofacies are commonly highly burrowed, suggesting deposition below a fair-weather wave base in a lower shore-face zone. Mollusks present in samples from the pelecypod-rich lithofacies are

suggestive of the outer estuary to shallow-marine platform interior environments of Florida Bay (Table 1).

Two lithofacies, peloid wackestone and packstone, and peloid packstone and grainstone, characterize the Miami Limestone (Figs. 3 and 4). Burrowing of these lithofacies is pervasive, suggesting deposition below a fair-weather wave base in a lower shore-face zone. A benthic foraminiferal assemblage dominated by archaiasinids, soritids, and peneroplids in the peloid wackestone and packstone lithofacies is consistent with deposition in an open-marine platform interior (Rose and Lidz, 1977; Lidz and Rose, 1989). *Schizoporella* bryozoan are commonly present in both lithofacies. The two lithofacies correspond to the bryozoan facies of Hoffmeister et al. (1967), which they interpreted to represent an open-marine shelf lagoon. Later, both Perkins (1977) and Evans (1984) indicated deposition of the bryozoan facies was on an open-marine platform.

Restricted Platform Interior

Characteristic of the restricted platform interior environment is typical pelecypod floatstone and rudstone, sandy pelecypod floatstone and rudstone, skeletal packstone and grainstone, and sandy skeletal packstone and grainstone lithofacies. Miliolids commonly dominate the benthic foraminiferal assemblage of the lithofacies, which is consistent with deposition in a restricted platform interior. Lidz and Rose (1989), and Rose and Lidz (1977) noted that miliolid-dominated benthic foraminiferal assemblages are common in restricted areas of modern Florida Bay. These lithofacies are commonly highly burrowed, suggesting deposition below a fair-weather wave base in a lower shore-face zone.

Brackish Platform Interior

The mudstone and wackestone lithofacies commonly distinguishes the brackish interior platform environment. This lithofacies is principally micrite and has an abundance of the benthic foraminifer *Ammonia* and smooth-shelled ostracods. Charophytes, the benthic foraminifer *Elphidium*, and the freshwater gastropod *Planorbella* are less commonly present. Other types of benthic foraminifers are not common. Modern Florida Bay sediments with large populations of *Ammonia* and *Elphidium*, and containing few other foraminiferal species, are indicative of a brackish platform interior (Rose and Lidz, 1977; Lidz and Rose, 1989).

Freshwater Terrestrial

The *Planorbella* floatstone and rudstone lithofacies characterizes a freshwater terrestrial environment. This micrite-rich lithofacies commonly contains abundant *Planorbella*, smooth-shelled ostracods, and charophytes. Interpretation indicates deposition of the *Planorbella*-rich beds in freshwater ponds or marshes (Galli, 1991).

CYCLOSTRATIGRAPHY

The cyclostratigraphy presented herein divides fundamental depositional cycles (high-frequency cycles) into units defined by distinct vertical lithofacies successions bounded by surfaces across which there is evidence for a relative increase in sea level (cf. Kerans and Tinker, 1997). Relative changes in sea level can have significant control over vertical patterns of the stacking of lithofacies on carbonate platforms (Kerans and Tinker, 1997). Although the concept of sea-level control on cycle production has been challenged (Miall, 1997; Drummond and Wilkinson, 1993), the systematic application of cyclostratigraphy has been shown to be an effective approach for defining stratigraphic and petrophysical (porosity and permeability) spatial relations (Hovorka et al., 1996, 1998; Lucia, 1999; Budd, 2001; Ward et al., 2003; Budd and Vacher, 2004; Cunningham et al., 2004b, 2004c, 2006). It is not our purpose to determine whether high-frequency cycles have a eustatic (e.g., Perkins,

TABLE 1. IDEAL CYCLES OF THE FORT THOMPSON FM AND MIAMI LIMESTONE AT THE NORTHWEST WELL FIELD

Cycle type	Major depositional environments	Description
Aggradational subtidal cycle	Open-marine platform interior environment	Cycle thickness range 0.1-1.0 m, mean 0.6 m. Little or no change in grain size upward through succession. Mainly peloid packstone and grainstone or peloid wackestone and packstone lithofacies. Top of upper boundary is an exposure surface (calcrete).
Upward-shallowing paralic cycle	Open-marine platform interior, restricted platform interior, brackish platform interior, and freshwater terrestrial environments	Cycle thickness range 0.5-4.0 m, mean 1.8 m. Fining upward succession. Base typically burrowed pelecypod-rich floatstone or rudstone lithofacies, which may be quartz sand rich, grading upward to mudstone and wackestone or *Planorbella* floatstone and rudstone cap. Half of cycles have an exposure surface at upper boundary (calcrete). *Planorbella* present in capping *Planorbella* floatstone and rudstone lithofacies, and local occurrence in mudstone and wackestone lithofacies. Mollusks present in the middle to lower part of the cycle include *Anodontia alba*, *Cerithium* sp. (cf., *C. viciinia*), *Chione cancellata*, *Codakia orbicularis*, *Conus* sp., *Lithopoma americanum*, *Modulus modulus*, *Oliva* sp., pectinids, *Phacoides* (*Bellucina*) *waccamawensis*, *Trachycardium* sp. (cf., *T. muricatum*), *Turbo castanea*, *Divaricella compsa*, *Dosinia nassula*, *Astralium phoebium*, *Lucinisca nassula*, *Turritella subannulata*, *T. apicalis*, *Glycymeris* sp., *Strombus* sp.
Upward-shallowing subtidal cycle	Open-marine platform interior and restricted platform interior environments	Cycle thickness range 0.4-3.5 m, mean 1.7 m. Mostly fining upward succession. Base typically burrowed pelecypod-rich floatstone or rudstone, which may be quartz sand rich, grading upward to packstone and grainstone. One-third of cycles have an exposure surface at upper boundary (calcrete). Mollusks present in cycles include *Chione cancelleta*, *Trachycardium egmontium*?, *Trachycardium* sp., *Nuculana acuta*, *Turritella subannulata*, *Parastarte triquetra*.

1977; Multer et al., 2002) or autocyclic origin, since this study includes only a very small part of the lateral extent of the Fort Thompson Formation and Miami Limestone.

Delineation of Cycles and Ideal Cycles

High-frequency cycles form the fundamental building blocks of the rocks of the Biscayne aquifer (Figs. 3, 4, and 6). The placement of vertical lithofacies successions between significant bounding surfaces defines these cycles (Fig. 3). Bounding surfaces are flooding surfaces. In some cases, a calcrete layer indicative of subaerial exposure delineates the flooding surface (Fig. 4). A flooding surface is a boundary that separates younger from older strata and across which there is a sharp upward increase in paleowater depth (cf. Van Wagoner et al., 1988). Flooding surfaces herein indicate a sharp upward deepening of paleomarine water depth or paleoflooding of a subaerial exposure surface by seawater or freshwater.

Three distinct recurring vertical lithofacies successions translate into three ideal high-frequency cycles: an upward-shallowing subtidal cycle, an upward-shallowing paralic cycle, and an aggradational subtidal cycle (Fig. 3; Table 1). Paralic depositional facies cap the upward-shallowing paralic cycles. The principal characteristic of paralic environments is that they occur at the transition between marine and terrestrial realms—estuaries, coastal lagoons, marshes, and coastal zones subject to high freshwater input (Debenay et al., 2000). Figure 3 shows the vertical stacking of lithofacies and associated interpretive depositional environments within the three ideal high-frequency cycles. In the Fort Thompson Formation, only the two upward-shallowing cycles were observed, and only aggradational subtidal cycles were observed in the Miami Limestone (Fig. 4).

Cycle Hierarchy

In the Fort Thompson Formation and Miami Limestone, two hierarchical levels of cyclicity were observed. The high-frequency cycles are the fundamental cycle type, but based on upward trends of progradation or aggradation, they group into two high-frequency cycle sets (Fig. 4; Table 2). The lower high-frequency cycle set (Fort Thompson Formation) displays a broad uniform upward-shallowing trend indicative of carbonate-shelf progradation. The singular depositional facies characteristic of the two high-frequency cycles of the upper high-frequency cycle set (Miami Limestone) is suggestive of carbonate-shelf aggradation (cf. Kerans and Tinker, 1997).

Orders of Cycles

Within the study area, we propose a hierarchical order to the cyclicity recognized in the Fort Thompson Formation and Miami Limestone: high-frequency cycles are fifth-order scale and high-frequency cycle sets are fourth-order scale (Table 2). The proposed scales for the cycle ordering are based on various ranges of ages proposed by Multer et al. (2002) for the five unconformity-bound Quaternary marine units or Q units defined by Perkins (1977). Perkins' (1977) Q1–5 units correlate to our new cyclostratigraphy shown in Figure 4, based on comparison of his descriptions of lithofacies and unconformities to those we observed. No lithofacies or unconformity observed in the study area reliably correlated to Perkins' Q1 unit (Fig. 4). Multer et al. (2002) assumed a maximum age of 420 ka for Perkins' Q1 unit (basal Fort Thompson Formation; Fig. 2) and reported that the Q5 unit of Perkins (1977) accumulated during the marine isotope substage 5e, which terminated ca. 114 ka (Shackleton et al., 2003). Our model of the ordering of cyclicity thus assumes a maximum duration of ~306 k.y. for accumulation of the 13 high-frequency cycles identified in the study area (Fig. 4), or an average cycle duration of ~23.5 k.y., which is consistent with fifth-order cyclicity (Table 2). Fourth-order scaling of the high-frequency cycle sets is in agreement with cycle-set durations based on Q-unit ages presented in Perkins (1977) and Multer et al. (2002).

PORE CLASSES

The porosity and permeability in the Biscayne aquifer are related to lithofacies and have a predictable vertical distribution within the upward-shallowing cycles of the Fort Thompson Formation and the aggradational subtidal cycles of the Miami Limestone (Cunningham et al., 2004b, 2006). Each of the 15 lithofacies of the Fort Thompson Formation and Miami Limestone in the study area has been assigned to one of three pore classes (I, II, and III), as shown in Table 3. These lithofacies have rather unique stratigraphic spatial distributions, and porosity and permeability characteristics.

Pore class I commonly includes the lower part of many of the upward-shallowing cycles within the Fort Thompson Formation and upper aggradational subtidal cycle of the Miami Limestone, where the porosity and permeability are highest (Figs. 3 and 6; Table 3). Characteristic lithofacies associated with pore class I are (1) touching-vug pelecypod rudstone and floatstone, (2) sandy touching-vug pelecypod rudstone and floatstone, (3) peloidal packstone and grainstone, (4) coral framestone, and (5) laminated peloid packstone and grainstone lithofacies (Table 3). Pore types commonly associated with specific lithofacies include solution-enlarged fossil molds up to pebble size, irregular vugs of uncertain origin, and molds of burrows or roots, or irregular vugs surrounding casts of burrows or roots (Fig. 7). Touching-vugs are the most common type of effective porosity in this class, but conduit porosity also occurs as bedding-plane vugs and uncommon cavernous vugs (Cunningham et al., 2006). A tabular three-dimensional geometry regionally characterizes the touching-vug flow zones, which are constrained between cycle boundaries, based on porous-zone mapping in the Lake Belt area (e.g., Cunningham et al., 2004b, 2004c, 2006). Therefore, accurate cycle correlation can produce a realistic linkage of permeable or preferential groundwater flow

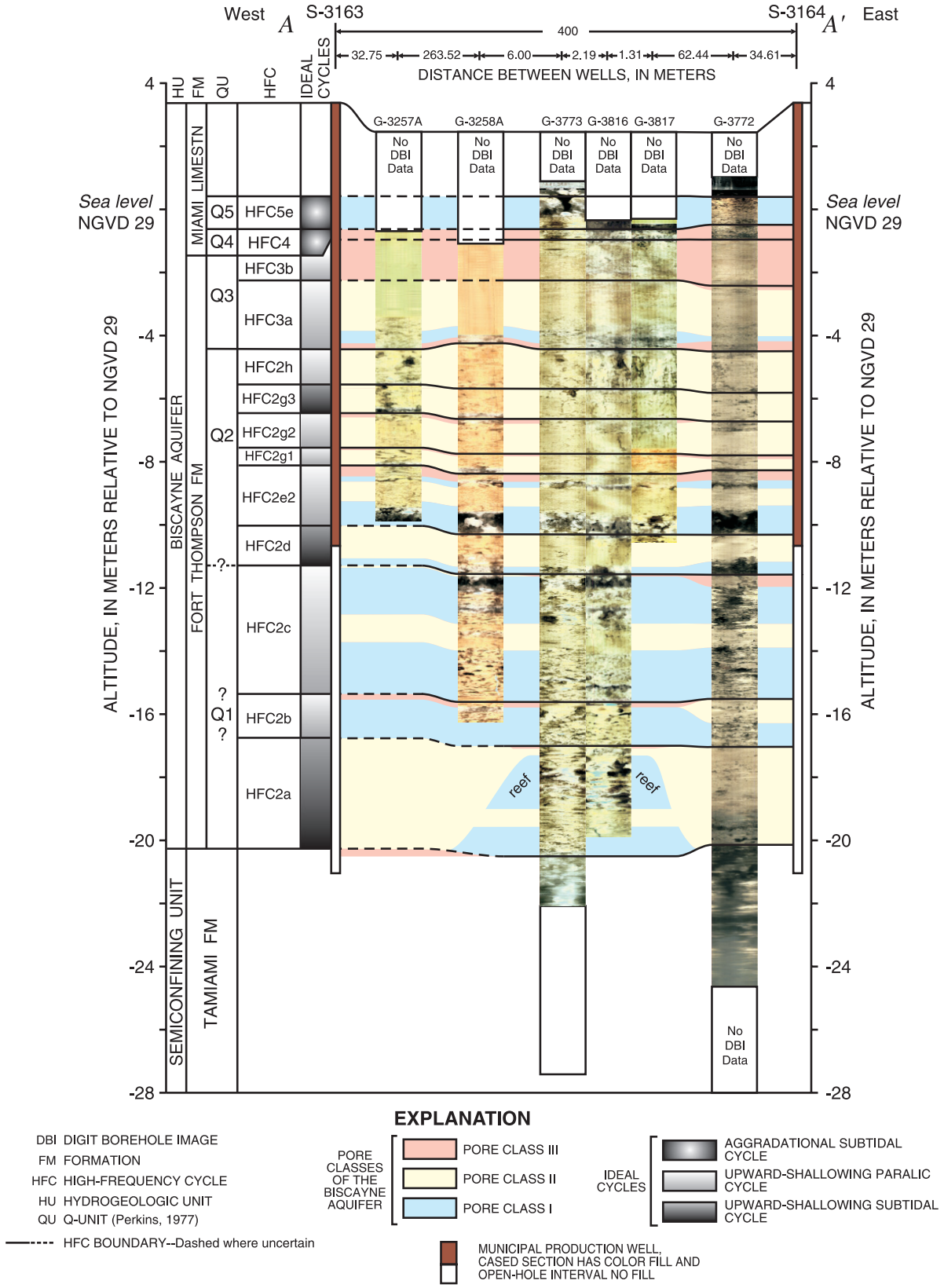

Figure 6. Hydrostratigraphic correlation section A–A′ between the S-3163 and S-3164 production wells, including six digital optical image logs from observation and injection wells at the Northwest Well Field (Fig. 1D). Black or very dark areas on the digital optical image logs commonly indicate large-scale vuggy porosity.

zones. Groundwater flow in the touching-vug flow zones should not be conceptually viewed as the movement of groundwater through a system of large-scale pipes or underground stream conduits, but more of a stratiform passage formed by coalescence of vugs into a mostly tortuous path for the movement of groundwater flow from vug to vug (Fig. 3). Figure 6 best exemplifies the stratiform distribution of pore class I, notably in digital optical borehole images where the darkened area at the base of high-frequency cycle HFC2e2 represents touching-vug porosity (Fig. 7). Cunningham et al. (2004b, 2006) showed that pore class I has the highest porosity and permeability of the three pore classes defined herein.

Typically assigned to pore class II are the (1) skeletal packstone and grainstone, (2) sandy skeletal packstone and grainstone, (3) pelecypod floatstone and rudstone, (4) sandy pelecypod floatstone and rudstone, and (5) skeletal quartz sandstone lithofacies (Table 3). The first four lithofacies listed commonly occur in the upper part of upward-shallowing subtidal cycles and the middle part of the upward-shallowing paralic cycles (Fig. 3), and the last lithofacies is uncommon. Interparticle and separate-vug porosity characterize these lithofacies, which yield groundwater movement through vug-to-matrix-to-vug connections (Lucia, 1999). Diffuse-carbonate groundwater flow (cf. Shuster and White, 1971; Thrailkill, 1976) characterizes movement of groundwater in areas of the Biscayne aquifer characterized by pore class II (Fig. 3).

Usually assigned to pore class III are (1) mudstone and wackestone, (2) *Planorbella* floatstone and rudstone, (3) peloid wackestone and packstone, (4) conglomerate, and (5) pedogenic limestone lithofacies (Table 3). The first two lithofacies commonly cap upward-shallowing paralic cycles, and the third and fourth are representative of the lower aggradational subtidal cycle of the Miami Limestone (Fig. 3). Porosity types common to this pore class include thin, semivertical solution pipes, and fossil molds. The matrix porosity and permeability of these lithofacies are low (Table 3), and the solution pipes (small-scale conduits) and fossil molds are typically unconnected. Thus, these lithofacies tend to retard groundwater movement and are conceptualized as leaky, low-permeability units (Fig. 3). On a local scale, however, pore class III can comprise bedding-plane vugs, which may have sheet-like geometry and could represent major conduits that are highly permeable.

TABLE 2. TERMINOLOGY OF STRATIGRAPHIC CYCLE HIERARCHIES AND ORDERS OF CYCLICITY

Order	Sequence stratigraphic unit	Duration (my)
First	--	>100
Second	Supersequence	10–100
Third	Depositional sequence, composite sequence	1–10
Fourth	High-frequency sequence, high-frequency cycle set	0.1–1
Fifth	High-frequency cycle	0.01–0.1

Note: Kerans and Tinker (1997).

EVIDENCE FOR FLOW-ZONE CONTINUITY

On 22 April 2003, a forced-gradient tracer test was performed using 50 kg of Rhodamine WT and 15 kg of deuterated water (Renken et al., 2005). The conservative tracers were introduced into the G-3773 injection borehole located ~100 m from the S-3164 municipal production well (Fig. 1D). The injection transpired in an open borehole that extended from ~10.2–20.0 m depth below land surface (Fig. 8). Tracer-free formation water was used as a chaser to insure dispersal of the conservative tracers away from the borehole. The principal

TABLE 3. PORE CLASSES (I, II, III) RELATED TO AQUIFER ATTRIBUTES AT THE NORTHWEST WELL FIELD

Pore class	Lithofacies	Major pore type	Approximate median whole-core porosity (Cunningham et al., 2004b)	Median maximum horizontal air permeability (Cunningham et al., 2004b)	Major groundwater-flow type and relative permeability
III	Mudstone-wackestone, *Planorbella* floatstone-rudstone, peloidal wackestone-packstone, conglomerate, and pedogenic limestone	Separate vugs including moldic porosity or thin vertical solution pipes or both	Aggradational subtidal cycle = 16% and cycle top of upward-shallowing paralic cycles = 16%	Aggradational subtidal cycle = 150 md and cycle top of upward-shallowing paralic cycles = 21 md	Leaky, low permeability
II	Skeletal packstone-grainstone, sandy skeletal packstone-grainstone, pelecypod floatstone-rudstone, sandy pelecypod floatstone-rudstone, and skeletal quartz sandstone	Matrix porosity including interparticle porosity and separate vugs	Middle or upper part of upward-shallowing cycles = 22%	Middle or upper part of upward-shallowing cycles = 130 md	Diffuse-carbonate flow, moderate permeability
I	Touching-vug pelecypod floatstone-rudstone, sandy touching-vug pelecypod floatstone-rudstone, peloid packstone-grainstone, coral framestone, and laminated peloid packstone-grainstone	Touching vug porosity including fossil-moldic, inter-burrow, burrow-moldic, and inter-root-cast, and root-moldic porosity, and irregular vugs; and conduit porosity including bedding-plane vugs and cavernous vugs	Aggradational subtidal cycle = 47% and lower part of upward shallowing cycles = 37%	Aggradational subtidal cycle = 1100 md and lower part of upward shallowing cycles = 1400 md	Touching-vug and less common conduit flow, high permeability

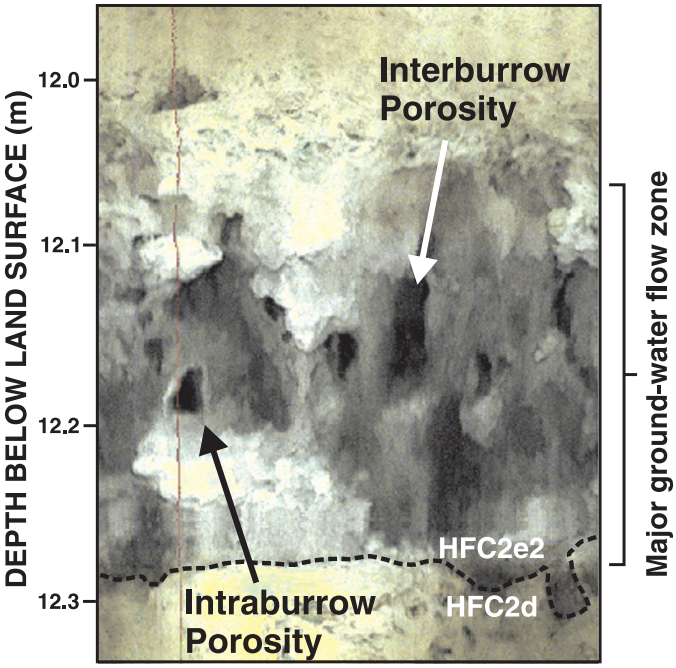

Figure 7. Digital image of a borehole wall that spans a highly porous and permeable stratiform groundwater flow zone at the base of high-frequency cycle HFC2e2 in injection well G-3816 (Figs. 4 and 6). Note intraburrow and interburrow porosity at arrows. The dashed line marks the boundary and flooding surface that separates high-frequency cycles HFC2d and HFC2e2.

objective was to quantitatively estimate formation properties that affect chemical transport and to aid the design of future particulate-tracer experiments.

In conjunction with the April 2003 conservative tracer test, fluid-temperature and fluid-conductivity borehole measurements were collected in the G-3772 observation well, located ~66 m from injection well G-3773 and ~34 m from the S-3164 production well (Fig. 1D). Borehole temperature and conductivity profiles were collected within the open-hole section of the G-3772 observation well at 102–322 min intervals as the tracer plume moved toward the production well (Fig. 8). An anomalous temperature change of ~0.8 °C was observed 3 h and 22 min (12:52 p.m. local time) after the completion of the tracer injection (Fig. 8). We assumed, for purposes of this discussion, that the liquid tracer (~210 L) had equilibrated to the average ambient air temperature (26 °C) on the day of the injection. Groundwater temperature on 22 April 2003 ranged from 22.5 to 23.5 °C. The observed 0.8 °C increase in fluid temperature at the observation well G-3772 was attributable to movement of the tracer pulse as it passed the G-3772 well bore. This temperature anomaly was recorded ~3 h prior to peak breakthrough of the tracers at pumping well S-3164 and at about the same time the leading edge of the tracer pulse was first detected at well S-3164 (Fig. 9). The change in fluid temperature appears to have been greatest at a depth interval of ~12.2–12.8 m below land surface (Fig. 8). This depth corresponds to an apparent high-permeability flow zone characterized by touching-vug porosity. This zone is located at the base of high-frequency cycle HFC2e2 (Fig. 7), which is just above the flooding surface bounding the top of high-frequency cycle HFCd2 (Fig. 4). This observation corroborates our conceptual karst aquifer model, which links most high-permeability zones to the lower part of high-frequency cycles. A fluid-temperature anomaly in the G-3772 observation well (Fig. 1D) strongly suggests that a substantial part of the tracer moved through a relatively thin (0.6 m) flow zone at the base of high-frequency cycle HFC2e2 (Figs. 7 and 8). A comparison of fluid-temperature data with fluid-conductivity profiles is less persuasive. Conductivity of the Rhodamine tracer was greater than ambient groundwater at 12:52 and 14:33 p.m. local time, and appeared to be dispersed within the borehole section that includes high-frequency cycles HFC2a to HFC2g1 (Fig. 8), but it is unclear what controlled the measured changes in conductivity during the tracer test.

Stationary and trolling electromagnetic flow-meter data obtained during ambient and pumping measurements at injection well G-3773 (Fig. 8) were collected in October 2003. Results suggest that under stressed conditions, significant movement of groundwater occurs at the base of high-frequency cycle HFC2e2, which is consistent with the borehole fluid temperatures collected during the tracer test. Uncertainty of the amount of fluid flow bypassing the flexible-disk diverter on the flow meter limits the accuracy of the measurements (Paillet, 2004).

DISCUSSION: BISCAYNE AQUIFER PORE SYSTEM AND EVOLUTION

Karst aquifers are traditionally characterized by three types of porosity: interparticle matrix porosity, fracture porosity, and large cavernous porosity (Martin and Screaton, 2001). This has led many to view karst aquifers as two-component systems, where much of the groundwater storage occurs in the matrix porosity or fractures or both, and transport of groundwater takes place in large dissolutional conduits (cf. Martin and Screaton, 2001). However, in young eogenetic karst, which defines the Pleistocene limestone of the Biscayne aquifer, a fourth porosity type, touching-vug porosity, is especially important in terms of conveyance of groundwater (Vacher and Mylroie, 2002; Cunningham et al., 2004b, 2006). The triple porosity of the Biscayne aquifer is typically a combination of (1) a matrix of interparticle and separate-vug porosity, providing much of the storage and, under dynamic conditions, diffuse-carbonate flow; (2) stratiform groundwater flow passageways formed by touching vugs; and, (3) less common, conduit porosity composed mainly of bedding-plane vugs, thin solution pipes, and cavernous vugs—pathways for conduit groundwater flow. Conduit and diffuse-carbonate groundwater flow occur within Tertiary limestone karst aquifers elsewhere; examples have been documented in the Yucatan aquifer (Mexico), the North Coast limestone aquifer (Puerto Rico), and the Floridan aquifer (USA) by Thrailkill (1976), Martin and Screaton (2001), Renken et al. (2002), and Ward et al.

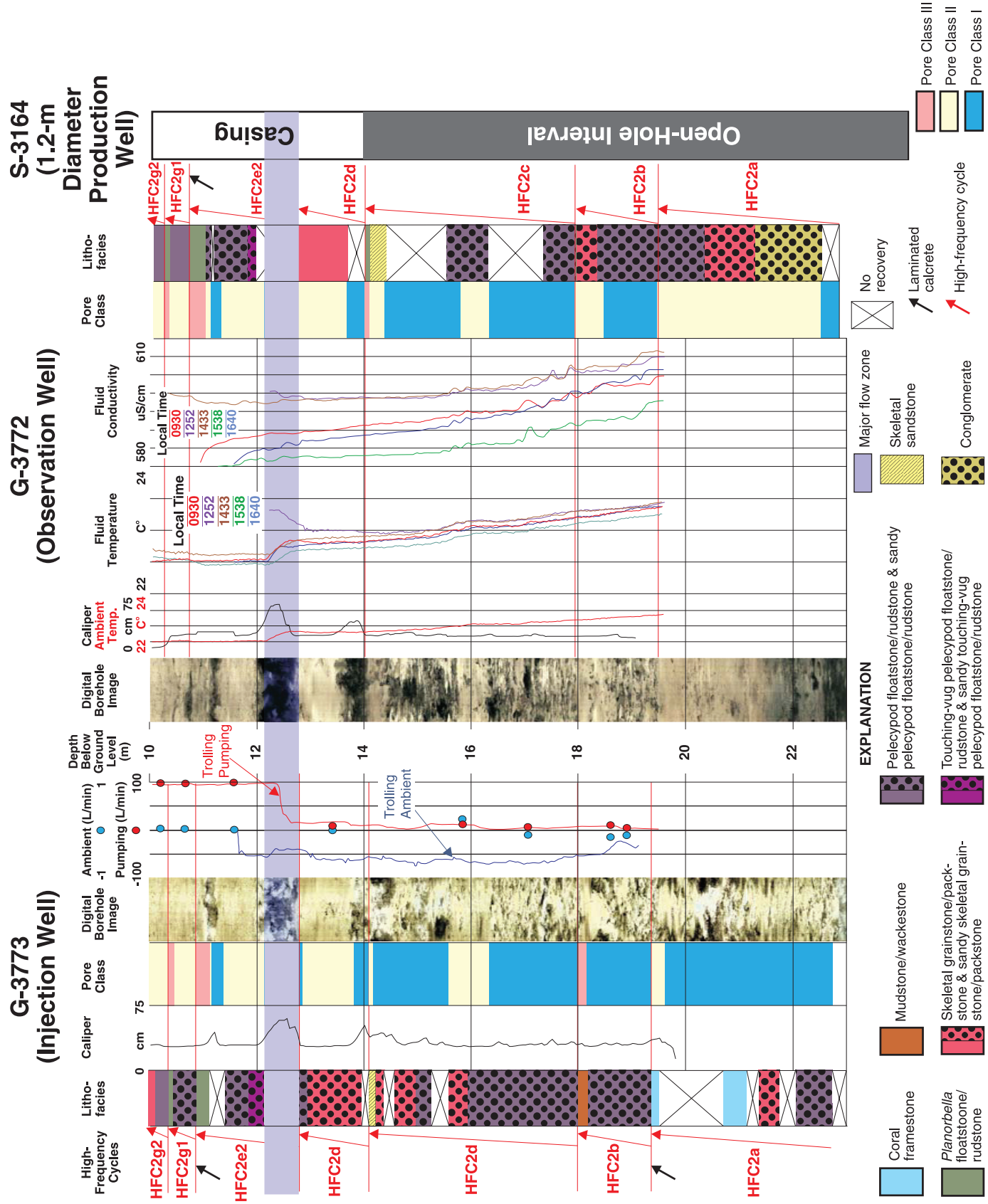
G-3773
(Injection Well)
G-3772
(Observation Well)
S-3164
(1.2-m
Diameter
Production
Well)
Casing
Open-Hole Interval
High-Frequency Cycles
Litho-facies
Caliper
Pore Class
Digital Borehole Image
Ambient (L/min)
Pumping (L/min)
Depth Below Ground Level (m)
Trolling Pumping
Trolling Ambient
Fluid Temperature
Fluid Conductivity
Local Time
0930
1252
1433
1538
1640
HFC2g2
HFC2g1
HFC2e2
HFC2d
HFC2c
HFC2b
HFC2a
No recovery
Laminated calcrete
High-frequency cycle
Major flow zone
Skeletal sandstone
Conglomerate
Pore Class III
Pore Class II
Pore Class I
EXPLANATION
Coral framestone
Mudstone/wackestone
Pelecypod floatstone/rudstone & sandy pelecypod floatstone/rudstone
Planorbella floatstoone/ rudstone
Skeletal grainstone/pack-stone & sandy skeletal grain-stone/packstone
Touching-vug pelecypod floatstone/ rudstone & sandy touching-vug pelecypod floatstone/rudstone

Figure 8. Correlation of cyclostratigraphy, lithofacies, pore classes, and borehole geophysical logs for injection well G-3773, observation well G-3772, and open hole interval of production well (S-3164) at Northwest Well Field (Fig. 1D). Major flow zone at the high-frequency cycle HFC2e2 base is shown as a horizontal blue stripe inferred from digital borehole images, flow-meter measurements, caliper, and fluid-temperature logs. Pumping flow-meter measurements were accomplished by pumping groundwater out of a cased borehole for well G-3773. Positive and negative flow-meter rates indicate upward and downward flow in the borehole, respectively.

(2003). Examples of touching-vug porosity in Pleistocene limestone karst aquifers have been discussed by Vacher and Mylroie (2002) and Cunningham et al. (2004b, 2006).

Our triple-porosity conceptual model of the karst Biscayne aquifer contains a series of vertically stacked interlayered (1) diffuse-carbonate flow zones, (2) touching-vug flow zones, and (3) less common conduit flow zones. Leaky, low-permeability zones are interbedded with some of the flow zones. Both high-permeability and low-permeability zones occur within the context of high-frequency cycles (Figs. 3 and 4). Visual examination of cores and digital borehole images (Figs. 5 and 6), quantification of porosity and permeability in cores (Table 3), computed porosity from digital borehole images (Cunningham et al., 2004b), and temperature and flow-meter logs (Fig. 8) indicate that permeability of the Biscayne aquifer is heterogeneous. The touching-vug flow in pore class I is mostly constrained to zones of solution-enlarged burrows, interburrow vugs, moldic fossils, root molds, or vugs between root casts that overprint repeating vertical arrangements of lithofacies within stacked high-frequency cycles. Touching-vugs characterize these secondary dissolution features, which coalesce to form tabular-like stratiform zones of vug-to-vug groundwater flow. The size, shape, and spatial distribution of touching-vug porosity within the Biscayne aquifer can be mapped within the context of the high-frequency cyclostratigraphic framework because they commonly occur in the lower part of the high-frequency cycles above flooding surfaces, which facilitates well-to-well interpolation of highly porous zones. These highly porous zones commonly occur at the base of the paralic and subtidal upward-shallowing cycles of the Fort Thompson Formation and throughout the uppermost subtidal aggradational cycle of the Miami Limestone (Figs. 3, 4, and 6).

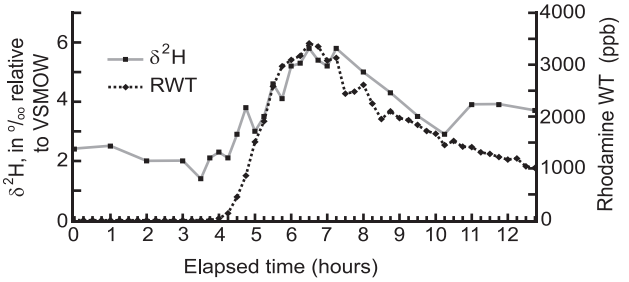

Figure 9. Graph showing breakthrough curves for two tracers, Rhodamine WT and deuterated water (δ^2H), based on groundwater samples collected from pumping well S-3164 during a tracer test conducted at the Northwest Well Field in April 2003 (Fig. 1D). The leading edge of the tracer pulse was detected ~3 h prior to peak breakthrough of the two tracers, which occurred 6.5 h after they were introduced into the G-3773 injection borehole (Fig. 1D). VSMOW—Vienna standard mean ocean water.

Small-scale interparticle and separate-vug porosity mostly contributes to the diffuse-carbonate groundwater flow (flow through pore class II) in the Biscayne aquifer (cf. Shuster and White, 1971; Thrailkill, 1976; Martin and Screaton, 2001). These two pore types relate to specific lithofacies, and diffuse-carbonate flow is the principal type of flow in the middle of ideal paralic upward-shallowing cycles and the upper part of ideal subtidal upward-shallowing cycles of the Fort Thompson Formation (Fig. 3). Cunningham et al. (2004b) showed that in the upper Biscayne aquifer, median values of core-scale air permeabilities from the middle (diffuse) part of paralic upward-shallowing cycles are about one order of magnitude less than the lower part of these cycles, where the pore system is principally touching-vugs. However, the relative difference in median permeability values between diffuse-carbonate and touching-vug flow zones must be even greater because recovery of intact core samples has never been accomplished for the most porous and permeable parts of touching-vug zones at the base of cycles, where the limestone is fragile and always broken up during drilling. Thus, no laboratory measurements exist for core-scale permeabilities from the most permeable part of touching-vug flow zones, precluding comparison of core-scale touching-vug flow-zone permeabilities to known permeability values of core samples from diffuse-carbonate flow zones.

We propose that karstic development of the highly permeable zones at the base of upward-shallowing cycles of the Fort Thompson Formation relates to cyclostratigraphy and Pleistocene sea-level history. Figure 3 shows that the vertical arrangement of lithofacies and pore classes are linked within the context of ideal high-frequency cycles. Formation of secondary porosity was likely produced by meteoric water flowing through the limestone of the Fort Thompson Formation during its emergence into the vadose zone, caused by periodic lowstands in sea level that span Pleistocene glacial maximums (Perkins, 1977). It is possible that these episodic vadose events promoted aggressive dissolution of carbonate grains and depositional textures in the lower part of cycles due to perched, concentrated, downdip flow of meteoric water above flooding surfaces. We hypothesize the focusing of low-gradient, lateral flow of meteoric water above flooding surfaces was due to the presence of relatively low-permeability lithologies at cycle tops, which underlie the flooding surfaces and act as baffles or barriers to downward vertical drainage.

CONCLUSIONS

A fundamental problem in the simulation of karst groundwater flow and solute transport is how best to represent aquifer heterogeneity as defined by the spatial distribution of porosity

and permeability. By combining analyses of lithofacies, depositional environments, cyclostratigraphy, and borehole geophysical logs as they relate to porosity and permeability, we have improved the representation of the aquifer attributes of porosity and permeability within the triple-porosity (matrix, touching-vug, and conduit porosity) karst Biscayne aquifer in a 0.65 km^2 study area in SE Florida.

Rock fabric and texture, faunal constituents, sedimentary structures, and relation to surfaces bounding vertical lithofacies successions were the basis for our definitions of five principal depositional environments for the Pleistocene Fort Thompson Formation and Miami Limestone, the major lithologic components of the Biscayne aquifer. The five depositional environments are (1) platform margin to outer platform, (2) open-marine platform interior, (3) restricted platform interior, (4) brackish platform interior, and (5) freshwater terrestrial environments. Vertical lithofacies successions, which have stacking patterns that reoccur, fit within high-frequency cycles. Upward-shallowing subtidal cycles, upward-shallowing paralic cycles, and aggradational subtidal cycles define three types of ideal high-frequency cycles. Fundamental to the identification of an upward-shallowing paralic cycle is a capping micrite-rich carbonate lithology indicative of deposition in a paralic transitional realm between subaqueous brackish and terrestrial environments. Grouping of high-frequency cycles based on vertical cycle patterns produced two cycle sets, one progradational (Fort Thompson Formation) and another aggradational (Miami Limestone).

There is a predictable vertical pattern of porosity and permeability within the three ideal cycles, because the distribution of porosity and permeability relates directly to lithofacies. Fifteen major lithofacies of the Fort Thompson and Miami Limestone have been assigned to one of three pore classes (I, II, and III), as shown in Table 3. Pore class I commonly includes the lower part of upward-shallowing cycles within the Fort Thompson Formation and an upper aggradational cycle of the Miami Limestone. Vug-to-vug groundwater flow is most typical of pore class I. Conceptualization of the touching-vug flow is movement of groundwater through a stratiform passage formed by coalescence of vugs into a mostly tortuous path. Less common in pore class I is conduit groundwater flow through bedding-plane vugs and cavernous conduits. Pore class II commonly occurs in the upper part of the upward-shallowing subtidal cycles and middle part of the upward-shallowing paralic cycles. It is principally composed of interparticle and separate-vug porosity and characterized by diffuse-carbonate groundwater flow through vug-to-matrix-to-vug connections. Micrite-dominated lithologies distinguish pore class III, which commonly caps upward-shallowing paralic cycles and occurs throughout much of a lower aggradational cycle of the Miami Limestone. These lithologies tend to retard groundwater movement and are conceptualized as leaky, low-permeability units.

Zones of stratiform, high (but variable) permeability occur within many individual cycles and comprise preferential groundwater flow zones. Highly permeable zones commonly occur just above flooding surfaces in the lower part of upward-shallowing subtidal and paralic cycles. Aggradational subtidal cycles are either mostly high-permeability zones or leaky, low-permeability units. In the study area, groundwater flow within high-permeability zones is through a secondary pore system of stratiform touching-vug porosity principally related to molds of burrows and pelecypods, and to interburrow vugs. Movement of a dye-tracer pulse observed using a borehole fluid-temperature tool during a conservative tracer test indicates heterogeneous permeability. Advective movement of the tracer appears to have been most concentrated within a thin stratiform flow zone contained within the lower part of a high-frequency cycle, indicating a distinctly high relative permeability for this zone. Borehole flow-meter measurements corroborate the relatively high permeability of the flow zone. Identification and mapping of such high-permeability flow zones are crucial to conceptualization of karst groundwater flow within a cyclostratigraphic framework.

The cyclostratigraphic approach taken herein demonstrates (locally) that its combined use with borehole geophysical logs is valuable to the development of an accurate conceptual hydrogeologic model. The one-dimensional cyclostratigraphic framework, or fingerprint, of each well permitted discrete correlation of vertical lithofacies successions and high-frequency cycles, and the well-to-well connection of corresponding high-permeability zones between wells. The concepts should be useful for providing a framework for regional-scale triple- and dual-porosity groundwater-flow and solution-transport numerical simulations. Many karst aquifers occur in cyclic platform carbonates, so the cyclostratigraphic approach is applicable to many areas in the world (e.g., Hovorka et al., 1996, 1998; Ward et al., 2003; Cunningham et al., 2004b, 2006). Applications include well-head protection at well fields, design of tracer studies, solute-transport modeling of contaminants, saltwater intrusion modeling and monitoring in coastal areas, engineering design of underground barriers to seepage and tunnels, delineation of storage zones for aquifer storage and recovery projects, and providing a conceptual framework for development of next-generation simulations of regional karst groundwater flow.

ACKNOWLEDGMENTS

This study was funded as part of a cooperative agreement between the U.S. Geological Survey and the Miami-Dade County Department of Environmental Resource Management, and received grant funding from the American Water Works Association Research Foundation. The Miami-Dade County Water and Sewer Department graciously provided additional financial support and in-kind services. We thank T. Harrison, M. Stewart, and V. Walsh for their field assistance during the April 2003 tracer test. J. Baker, H. Guha, C. Oakley, and W. Pitt provided administrative guidance and technical support during the study. J. Williams and A. Anderson provided valuable

assistance during borehole flow-meter measurements. G. Shinn and Al Hine provided early technical reviews, and M. Deacon two editorial reviews. Constructive reviews by M. Grammer and an anonymous reviewer improved the manuscript.

Disclaimer: The use of firm, trade, and brand names in this report is for identification purposes only and does not constitute endorsement by the authors or their agencies.

REFERENCES CITED

Abbott, R.T., 1974, American seashells (2nd edition): New York, Van Nostrand Reinhold Company, 663 p.

Andrews, J.O., 1977, Shells and shores of Texas: Texas, Kingsport Press, 365 p.

Bock, W.D., Lynts, G.W., Smith, S., Wright, R., Hay, W.W., and Jones, J.I., 1971, A symposium of recent south Florida foraminifera: Miami, Florida, Miami Geological Society Memoir 1, 245 p.

Brewster-Wingard, G.L., Stone, J.R., and Holmes, C.W., 2001, Molluscan faunal distribution in Florida Bay, past and present: An integration of downcore and modern data: Bulletins of American Paleontology, v. 361, p. 199–231.

Budd, D.A., 2001, Permeability loss with depth in the Cenozoic carbonate platform of west-central Florida: American Association of Petroleum Geologists Bulletin, v. 85, p. 1253–1272.

Budd, D.A., and Vacher, H.L., 2004, Matrix permeability of the confined Floridan aquifer, Florida, USA: Hydrogeology Journal, v. 12, p. 531–549, doi: 10.1007/s10040-004-0341-5.

Cunningham, K.J., Carlson, J.I., and Hurley, N.F., 2004a, New method for quantification of vuggy porosity from digital optical borehole images as applied to the karstic Pleistocene limestone of the Biscayne aquifer, southeastern Florida: Journal of Applied Geophysics, v. 55, p. 77–90, doi: 10.1016/j.jappgeo.2003.06.006.

Cunningham, K.J., Carlson, J.L., Wingard, G.L., Robinson, E., and Wacker, M.A., 2004b, Characterization of aquifer heterogeneity using cyclostratigraphy and geophysical methods in the upper part of the karstic Biscayne aquifer, southeastern Florida: U.S. Geological Survey Water-Resources Investigation Report 03-4208, 46 p.

Cunningham, K.J., Wacker, M.A., Robinson, E., Gefvert, C.J., and Krupa, S.L., 2004c, Hydrogeology and ground-water flow at Levee 31N, Miami-Dade County, Florida, July 2003 to May 2004: U.S. Geological Survey Scientific Investigations Map I-2846, 1 sheet.

Cunningham, K.J., Wacker, M.A., Robinson, E., Dixon, J.F., and Wingard, G.L., 2006, A cyclostratigraphic and borehole geophysical approach to development of a three-dimensional conceptual hydrogeologic model of the karstic Biscayne aquifer, southeastern Florida: U.S. Geological Survey Scientific Investigations Report 2005-5235 (in press).

Debenay, J.-P., Guillou, J.-J., Redois, F., and Geslin, E., 2000, Distribution trends of foraminiferal assemblages in paralic environments: A base for using foraminifera as bioindicators, *in* Martin, R.E., ed., Environmental micropaleontology: The application of microfossils to environmental geology: Topics in Geobiology, v. 15, p. 39–67.

Drummond, C.N., and Wilkinson, B.H., 1993, Carbonate cycle stacking patterns and hierarchies of orbitally forced eustatic sea level change: Journal of Sedimentary Petrology, v. 63, p. 369–377.

DuBar, J.R., 1958, Stratigraphy and paleontology of the late Neogene strata of the Caloosahatchee River area of southern Florida: Florida Geological Survey Bulletin, v. 40, 267 p.

Dunham, R.J., 1962, Classification of carbonate rocks according to depositional textures, *in* Ham, W.E., ed., Classification of carbonate rocks: American Association of Petroleum Geologists Memoir 1, p. 108–121.

Embry, A.F., and Klovan, J.E., 1971, A late Devonian reef tract on Northeastern Banks Island, N.W.T.: Bulletin of Canadian Petroleum Geology, v. 19, p. 730–781.

Evans, C.C., 1984, Development of an ooid sand shoal complex: The importance of antecedent and syndepositional topography, *in* Harris, P.H., ed., Carbonate sands—A core workshop: Society of Economic Paleontologists and Mineralogists Core Workshop 5, p. 392–428.

Federal Register Notice, May 10, 2000: Washington, D.C., U.S. Government Printing Office, v. 65, no. 91, p. 30,194–30,274.

Galli, G., 1991, Mangrove-generated structures and depositional model of the Pleistocene Fort Thompson Formation (Florida Plateau): Facies, v. 25, p. 297–314.

Harrison, R.S., Cooper, L.D., and Coniglio, M., 1984, Late Pleistocene carbonates of the Florida Keys, *in* Kaldi, J., Watts, N., and Harrison, G., eds., Carbonates in subsurface outcrop: Calgary, Alberta, Canadian Society of Petroleum Geologists, p. 291–306.

Hickey, T.D., 2004, Geologic evolution of south Florida Pleistocene-age deposits with an interpretation of the enigmatic rock ridge development [M.S. thesis]: St. Petersburg, Florida, University of South Florida, 125 p.

Hoffmeister, J.E., Stockman, K.W., and Multer, H.G., 1967, Miami Limestone of Florida and its recent Bahamian counterpart: Geological Society of America Bulletin, v. 79, p. 175–190.

Hovorka, S.D., Dutton, A.R., Ruppel, S.C., and Yeh, J.S., 1996, Edwards aquifer ground-water resources: Geologic controls on porosity development in platform carbonates, south Texas: The University of Texas at Austin, Bureau of Economic Geology Report of Investigations 238, 75 p.

Hovorka, S.D., Mace, R.E., and Collins, E.W., 1998, Permeability structure of the Edwards aquifer, south Texas—Implications for aquifer management: The University of Texas at Austin, Bureau of Economic Geology Report of Investigations 250, 55 p.

Kerans, C., and Tinker, S.W., 1997, Sequence stratigraphy and characterization of carbonate reservoirs: Society of Economic Paleontologists and Mineralogists Short Course Notes 40, 130 p.

Keys, W.S., 1990, Borehole geophysics applied to ground-water investigations: U.S. Geological Survey Techniques of Water-Resources Investigations, Book 2, Chapter E2, 150 p.

Lidz, B.H., and Rose, P.R., 1989, Diagnostic foraminiferal assemblages of Florida Bay and adjacent shallow water: A comparison: Bulletin of Marine Science, v. 44, p. 399–418.

Lucia, F.J., 1995, Rock-fabric/petrophysical classification of carbonate pore space for reservoir characterization: American Association of Petroleum Geologists Bulletin, v. 79, p. 1275–1300.

Lucia, F.J., 1999, Carbonate reservoir characterization: New York, Springer-Verlag, 226 p.

Mansfield, W.C., 1939, Notes on the Upper Tertiary and Pleistocene mollusks of peninsular Florida: Florida Geological Survey Bulletin, v. 18, 75 p.

Martin, J.B., and Screaton, E.J., 2001, Exchange of matrix and conduit water with examples from the Floridan aquifer, *in* Kuniansky, E.L., ed., Proceedings of the U.S. Geological Survey Karst Interest Group: Water Resources-Investigations Report 01-4011, p. 38–44.

Miall, A.D., 1997, The geology of stratigraphic sequences: New York, Springer-Verlag, 433 p.

Multer, H.G., Gischler, E., Lundberg, J., Simmons, K.R., and Shinn, E.A., 2002, Key Largo Limestone revisited: Pleistocene shelf-edge facies, Florida Keys, USA: Facies, v. 46, p. 229–272.

Olsson, A.A., and Harbison, A., 1953, Pliocene mollusca of southern Florida: Academy of Natural Sciences of Philadelphia Monograph 8, p. 1–361.

Olsson, A.A., and Petit, R.E., 1964, Some Neogene mollusca from Florida and the Carolinas: Bulletins of American Paleontology, v. 47, p. 509–575.

Paillet, F., 2004, Borehole flowmeter applications in irregular and large-diameter boreholes: Journal of Applied Geophysics, v. 55, p. 39–59.

Perkins, R.D., 1977, Depositional framework of Pleistocene rocks in south Florida, *in* Enos, P., and Perkins, R.D., eds., Quaternary sedimentation in south Florida, part II: Geological Society of America Memoir 147, p. 131–198.

Perry, L.M., and Schwengel, J.S., 1955, Marine shells of the west coast of Florida: New York, Paleontological Research Institution, 318 p.

Poag, C.W., 1981, Ecologic atlas of benthic foraminifera of the Gulf of Mexico: New York, Academic Press, 174 p.

Portell, R.W., Schindler, K.S., and Morgan, G.S., 1992, The Pleistocene molluscan fauna from Leisey shell pit 1, Hillsborough County, Florida: Florida Geological Survey Special Publication, v. 36, p. 181–194.

Renken, R.A., Ward, W.C., Gill, I.P., Gómez-Gómez, F., Rodríguez-Martínez, J., Scharlach, R.A., Hartley, J.R., Hubbard, D.K., McLaughlin, P.P., and Moore, C.H., 2002, Geology and hydrology of the Caribbean Islands aquifer system of the Commonwealth of Puerto Rico and the U.S. Virgin Islands: U.S. Geological Survey Professional Paper 1419, 139 p.

Renken, R.A., Shapiro, A.M., Cunningham, K.J., Harvey, R.W., Metge, D.W., Zygnerski, M.R., Osborn, C.L., Wacker, M.A., and Ryan, J.N., 2005, Assessing the vulnerability of a municipal well field to contamination in a karst aquifer: Environmental and Engineering Geoscience, v. 11, p. 319–331.

Rose, P.R., and Lidz, B., 1977, Diagnostic foraminiferal assemblages of shallow-water modern environments: South Florida and the Bahamas: Miami, Florida, University of Miami, Sedimenta VI, 55 p.

Shackleton, N.J., Sanchez-Goni, M.F., Pailler, D., and Lancelot, Y., 2003, Marine isotope substage 5e and the Eemin interglacial: Global and Planetary Change, v. 36, p. 151–155, doi: 10.1016/S0921-8181(02)00181-9.

Shuster, E.T., and White, W.B., 1971, Seasonal fluctuations in the chemistry of limestone springs: A possible means for characterizing carbonate aquifers: Journal of Hydrology, v. 14, p. 93–128, doi: 10.1016/0022-1694(71)90001-1.

Thrailkill, J.V., 1976, Carbonate equilibrium in karst waters, *in* Proceedings, U.S.-Yugoslavian Symposium on Karst Hydrology and Water Resources, Dubrovnik, June 1975: Fort Collins, Colorado, Water Resources Publications, p. 745–771.

Vacher, H.L., and Mylroie, J.E., 2002, Eogenetic karst from the perspective of an equivalent porous medium: Carbonates and Evaporites, v. 17, p. 182–196.

Van Wagoner, J.C., Posamentier, H.W., Mitchum, R.M., Vail, P.R., Sarg, J.F., Loutit, T.S., and Hardenbol, J., 1988, An overview of the fundamentals of sequence stratigraphy and key definitions, *in* Wilgus, C.K., Hastings, B.J., Posamentier, H., Van Wagoner, J.C., Ross, C.A., and Kendall, C.G.St.C., eds., Sea-level change: An integrated approach: Society of Economic Paleontologists and Mineralogists Special Publication 42, p. 39–46.

Ward, W.C., Cunningham, K.J., Renken, R.A., Wacker, M.A., and Carlson, J.I., 2003, Sequence-stratigraphic analysis of the Regional Observation Monitoring Program (ROMP) 29A test corehole and its relation to carbonate porosity and regional transmissivity in the Floridan aquifer system, Highlands County, Florida: U.S. Geological Survey Open-File Report 03-201, 34 p., http://fl.water.usgs.gov/Abstracts/ofr03_201_ward.html.

Warmke, G.L., and Abbott, R.T., 1961, Caribbean seashells: Narberth, Pennsylvania, Livingston Publishing Co., 348 p.

White, W.B., 1999, Conceptual models for karstic aquifers, *in* Palmer, A.N., Palmer, M.V., and Sasowsky, I.D., eds., Karst modeling: Karst Waters Institute Special Publication, v. 5, p. 11–16.

White, W.B., 2002, Karst hydrology: Recent developments and open questions: Engineering Geology, v. 65, p. 85–105, doi: 10.1016/S0013-7952(01)00116-8.

White, W.B., and White, E.L., 2001, Conduit fragmentation, cave patterns, and localization of karst ground water basins: The Appalachians as a test case: Theoretical and Applied Karstology, v. 13–14, p. 9–23.

Manuscript Accepted by the Society 22 September 2005

Printed in the USA